Journal of Orthopaedic Translation 20 (2020) 100–106

Contents lists available at ScienceDirect

Journal of Orthopaedic Translation

journal homepage: www.journals.elsevier.com/journal-of-orthopaedic-translation

Original Article

Development of generic Asian pelvic bone models using CT-based 3D statistical modelling

Marc-Daniel Ahrend [a,b,*], Hansrudi Noser [a], Rukmanikanthan Shanmugam [c], Felix Burr [e], Lukas Kamer [a], Tunku Kamarul [d], Heinz Hügli [e], Andreas Nagy [e], Robert Geoff Richards [a], Boyko Gueorguiev-Rüegg [a]

[a] AO Research Institute Davos, Davos, Switzerland
[b] Department of Traumatology and Reconstructive Surgery, BG Trauma Center Tübingen, Eberhard Karls University Tübingen, Tübingen, Germany
[c] University of Malaya, Kuala Lumpur, Malaysia
[d] University of Malaya Medical Centre, Kuala Lumpur, Malaysia
[e] Synbone AG, Zizers, Switzerland

ARTICLE INFO

Keywords:
Bone models
Bone shape
Pelvic anatomy
Surgical education

ABSTRACT

Background/Objective: Artificial bone models (ABMs) are used in orthopaedics for research of biomechanics, development of implants and educational purposes. Most of the commercially available ABMs approximate the morphology of Europeans, but they may not depict the Asian anatomy. Therefore, our aim was to develop the first Asian ABM of the pelvis and compare it with the existing pelvic ABM (Synbone®; Caucasian male).

Methods: One hundred clinical computed tomography (CTs) of adult pelvises (male n = 50, female n = 50) of Malay, Chinese and Indian descent were acquired. CTs were segmented and defined landmarks were placed. Three 3D statistical pelvic model and mean models (overall, male, female) were generated. Anatomical variations were analysed using principal component analysis. To measure gender-related differences and differences to the existing ABM, distances between the anterior superior iliac spines (ASIS), the anterior inferior iliac spines (AIIS), the promontory and the symphysis (conjugate vera, CV) as well as the ischial spines (diameter transversa, DT) were quantified.

Results: Principal component analysis displayed large variability regarding the pelvic shape and size. Female and male statistical models were similar in ASIS (225 ± 20; 227 ± 13 mm; $P = 0.4153$) and AIIS (185 ± 11; 187 ± 10 mm; $P = 0.3982$) and differed in CV (116 ± 10; 105 ± 10 mm; $P < 0.0001$) and DT (105 ± 7; 88 ± 8 mm; $P < 0.0001$). Comparing the unisex mean model with the pre-existing ABM, the ASIS (226; 275 mm; $P < 0.0001$), the AIIS (186; 209 mm; $P < 0.0001$) and the CV (111; 105 mm; $P < 0.0001$) differed significantly. Both models were similar regarding DT (97; 95 mm; $P = 0.6927$). The analysis revealed notable gender- and size-dependent anatomical variations within the Asian population. Chinese, Malay and Indian descents did not differ notably. The overall Asian model was smaller than the existing ABM.

The translation potential of this article: Owing to the large differences between the Asian ABM and the pre-existing ABM, as well as differences between genders, the use of an Asian- and gender-specific ABM is important to consider in research, biomechanics and implant development for this population.

Introduction

Asia is experiencing a rapid growth in population. Its 50 countries and territories, with a population of approximately 4.3 billion people, account for 60% of the world population in total. Alongside the demographic change, trauma incidence and trauma care is increasing substantially for this region [1,2].

Artificial bone models (ABMs) are commonly used in traumatology and orthopaedics for biomechanical research, development and adjustment of implants and teaching purposes [3]. Predominantly made of polyurethane foam material, they represent a standardised cost-effective aid to teach osteosynthesis techniques and principles of fracture management, gain knowledge of bony landmarks for implant placement and develop dexterity in handling surgical tools and instruments [4,5]. It was

* Corresponding author. AO Research Institute Davos Clavadelerstr. 8 72070 Davos Switzerland.
E-mail address: marc@ahrend.de (M.-D. Ahrend).

https://doi.org/10.1016/j.jot.2019.10.004
Received 12 February 2019; Received in revised form 18 September 2019; Accepted 9 October 2019
Available online 4 November 2019

shown that the surgical ability of first-year residents improved because of training with bone models [6]. Furthermore, they may be utilised as an alternative to anatomical specimens because access, preparation and storage of the latter can be challenging and expensive [4,7]. To ensure proper usage, bone models need to depict the human anatomy accurately.

Comparative data demonstrated anatomical variations of different bones between the Asian and European ethnicities [8–12]. Regarding the pelvic region, Arima et al. [11] showed that Asians have a significant smaller pelvic incidence and a smaller sacral slope compared with Caucasians. Wagner et al. [12] showed that the Japanese pelvises have significant smaller diameters of S1 corridors resulting in more pelvises with a critical S1 corridor for trans-sacral implant positioning compared to Europeans. Most of the commercially available ABMs approximate the bone morphology of Europeans, but they may not sufficiently take into account the specific anatomical conditions of the Asian population. As a result, ABMs may be disproportionate and thus difficult to apply to Asians. Currently available models focus mainly on teaching the principals of fracture fixation without focussing on depicting the anatomy in detail. Until now, there is a substantial lack of an accurate scientific method to generate a precise anatomic model.

In the past years, we have extensively researched methods to generate three-dimensional (3D) statistical bone models using computed tomography (CT) data [13–17]. CT-based 3D statistical modelling represents a computerized technique that can demonstrate anatomical variation, as well as merging the anatomy of different individuals within a given anatomical region.

The objective of this study was to generate a three-dimensional statistical Asian bone model of the pelvis and to analyse shape and size variation within the population using principal component analysis (PCA) and linear measurements of the external and internal pelvic ring. Moreover, the aim was to subsequently manufacture a generic Asian pelvic ABM for research, development of implants and teaching purposes using CT-based 3D statistical modelling techniques and compare this novel Asian bone model with an existing artificial pelvic model. We hypothesised that significant differences can be found between the genders within the Asian population as well as between the novel Asian pelvic model and the existing pelvic model which, in our opinion, would justify the need for ethnicity-specific bone models for research, development and teaching purposes.

Materials and methods

Image data and software and hardware

One hundred clinical CT scans with intact pelvises of Malaysian adults (50 females, 50 males; age: 54.8 ± 16.4 years; body height: 161.3 ± 8.3 cm; body weight: 63.4 ± 14.8 kg) were acquired. They represented evenly distributed female and male patients of Malay, Chinese and Indian descent. The CT data were obtained during routine diagnostic procedures of the pelvis unrelated to this study with ethical approval from the respective local ethics committee (MREC ID N20159-1635). All CT scans were anonymized for study usage. Demographic data are summarised in Table 1. CT images with radiographic signs of bony pathologies (e.g. fractures, bone tumour or metastasis), unless age-related (e.g. osteoporosis, osteoarthritis), were excluded from the study. Only CTs displaying sacra with five fused sacral vertebrae and without spina bifida were considered for further processing.

Image data were acquired with multidetector CT scanners (Somatom, Definition AS+ and Definition, Siemens Healthcare GmbH, Erlangen, Germany; Ingenuity CT and Brilliance 4, Philips Healthcare, Cleveland, USA). CT scans were obtained using tube peak voltage set at 100–140 kVp and different reconstruction kernels (B20f, B26f, B30f, A, B, C, D). The image resolution was ≤1 mm (x axis 0.8 ± 0.1 mm, y axis 0.8 ± 0.1 mm and z axis 0.6 ± 0.2 mm). All CT image data were available in Digital Imaging and Communications in Medicine format with grey values given in Hounsfield units. They were transferred to a standard desktop computer and loaded to Amira, a commercial software package for scientific data visualisation and analysis (Amira software, version 6.3.0, Visualisation Science Group, FEI, Hillsboro, Oregon, USA).

Table 1
Demographic data of the collected 100 CT samples in terms of mean and standard deviation (SD) ([#]Unpaired t-test, [§]Mann–Whitney U test, °ANOVA with Tukey–Kramer post hoc test).

CT samples	N	Age [years]	Body height [cm]	Body weight [kg]
Total	100	54.8 ± 16.4 range: 19–83	161.3 ± 8.3 range: 145–188	63.4 ± 14.8 range: 31–122
Females	50	51.7 ± 16.9 range: 22–83	156.7 ± 5.9 range: 145–174	59.9 ± 11.8 range: 31–90
Males	50	57.9 ± 15.5 range: 19–81	166.0 ± 7.8 range: 150–188	66.7 ± 16.4 range: 38–122
		P = 0.0793[§]	*P < 0.0001*[#]	*P = 0.0159*[§]
Chinese	34	59.3 ± 15.8 range: 19–81	159.9 ± 7.6 range: 145–176	57.1 ± 11.0 range: 38–85
Indian	33	56.9 ± 17.6 range: 24–83	163.0 ± 10.0 range: 146–188	67.5 ± 14.8 range: 43–110
Malay	33	48.7 ± 14.8 range: 22–72	161.2 ± 7.0 range: 149–179	65.4 ± 16.1 range: 31–122
		P = 0.0214° *Chinese/Indian:* *P = 0.8168* *Chinese/Malay:* *P = 0.0219* *Indian/Malay:* *P = 0.0991*	*P = 0.3096*° *Chinese/Indian:* *P = 0.2781* *Chinese/Malay:* *P = 0.7812* *Indian/Malay:* *P = 0.6664*	*P = 0.0075*° *Chinese/Indian:* *P = 0.0087* *Chinese/Malay:* *P = 0.0466* *Indian/Malay:* *P = 0.8099*

ANOVA, analysis of variance.

CT data processing

CT data were processed according to a method described by Wagner et al. [16]. Standard threshold-based image segmentation was performed to generate 3D computer models of each pelvis. Anatomical homologous landmarks (38 on each innominate bone, 43 on the sacrum and 32 within the sacral foramina and the sacral canal) and nonhomologous segment landmarks were manually placed onto each pelvic bone model (Figure 1). Anatomical homologous landmarks represent anatomical points or bony prominences. The nonhomologous segment landmarks were used in regions with sharp edges and curvatures to connect the homologous landmarks. Nonhomologous landmarks were recomputed to obtain equally numbered and equidistant segment landmarks. Both sets of landmarks were selected according to Wagner et al. [16] and Arand et al. [18].

To produce a statistical form model of the pelvis, it is necessary to make all mesh models homologous, i.e., all computer models must have corresponding vertex and triangle numberings. As a reference, we first chose a typical pelvis model and remeshed it to get about 50 000 vertices for the sacrum and 50′000 vertices for each innominate bone. Thus, the entire pelvis comprising the innominate bones and the sacrum, including the neuroforamina and the medullary cavity is represented by 150′000 vertices. Next, this reference triangular mesh was warped onto the remaining 99 pelvises via thin plate spline transformation based on the homologous landmarks as described by Bookstein [19]. By a closest point method described by Noser et al. [13], the triangular mesh of the warped reference was then transferred to these pelvises. Thus, we obtained mesh homology for further statistical analysis such as statistical form generation or mean form computation. Before averaging the homologous triangular meshes, they were rigidly aligned to each other by a non-scaling general Procrustes fit algorithm (see also the study by Bookstein [17]). Iteratively, all homologous meshes are aligned to their common mean form by rigid transformations (without scaling and reflection) and minimising the overall alignment error. In the first step, the common

Figure 1. a) Axial two-dimensional (2D) CT reconstruction demonstrating segmentation of pelvic CTs with the innominate bones (green and yellow) and sacrum (purple) outlined; b) anterior view of the sacrum and medial view of the right innominate bone illustrating labelling via anatomical (red) and non-anatomical (yellow) landmarks; c) dorsal view of the sacrum and lateral view of the right innominate bone displaying homologous triangular meshed surfaces.

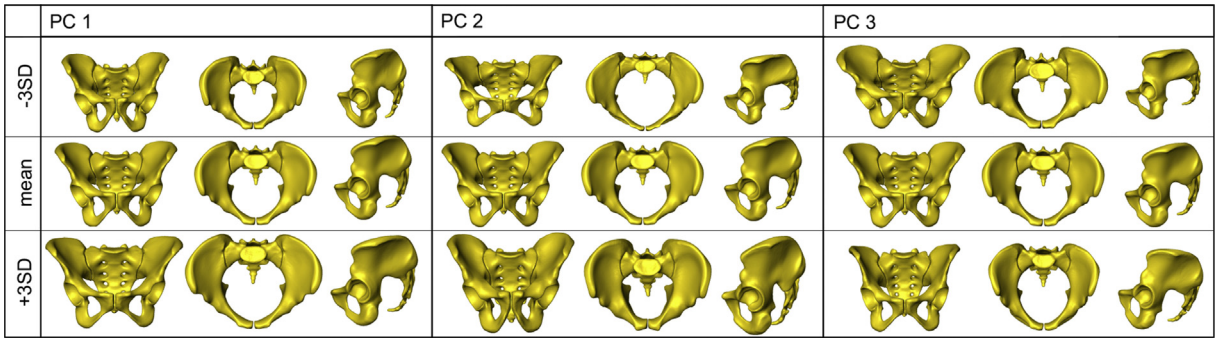

Figure 2. 3D statistical pelvic form model. Principal component analysis was applied to illustrate 3D shape and size variation. Mean model (middle row), PC 1, PC 2 and PC 3 as well as ±3SD models (top and bottom row) were visualised in anteroposterior, inlet and lateral views.

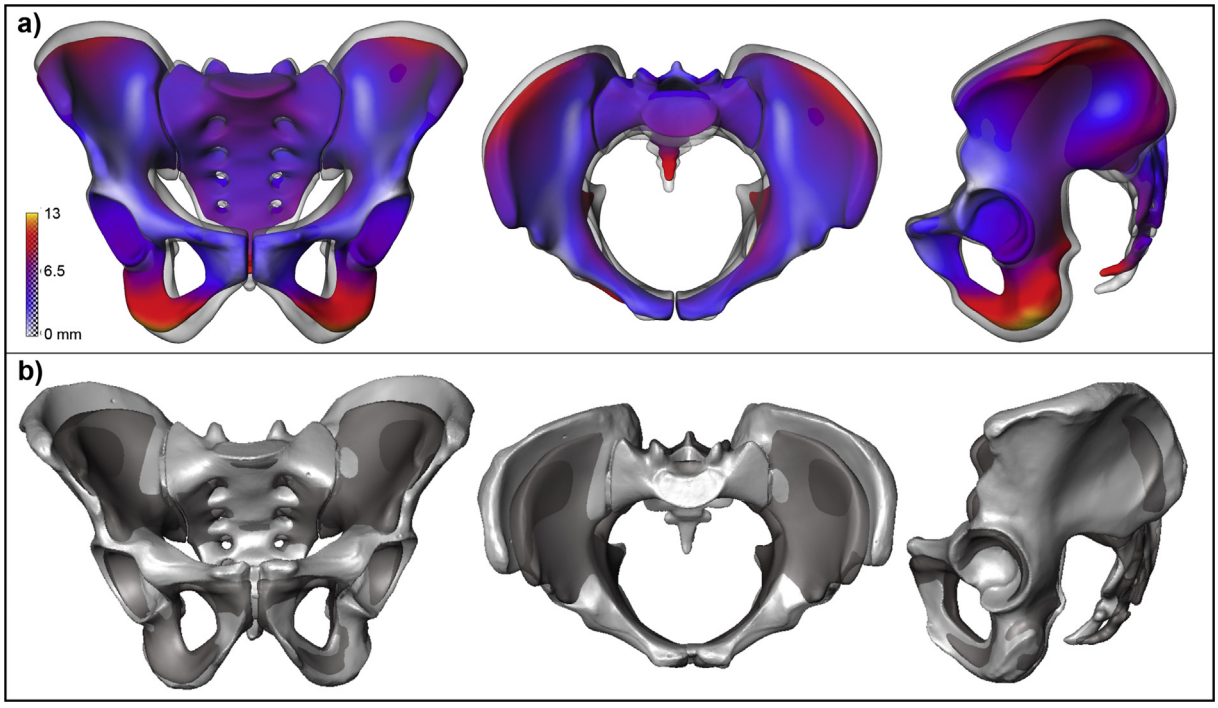

Figure 3. a) Qualitative and quantitative comparison of the distances between homologous points of the male pelvic mean model (grey transparent) versus female pelvic mean model (coloured) illustrated in anteroposterior, inlet and lateral. The colour map illustrates the differences of the distances in mm; b) qualitative comparison of the overall Asian pelvic mean model (dark grey transparent) and the pre-existing pelvic bone model (Synbone pelvic model no. 4060, light grey) in anteroposterior, inlet and lateral view.

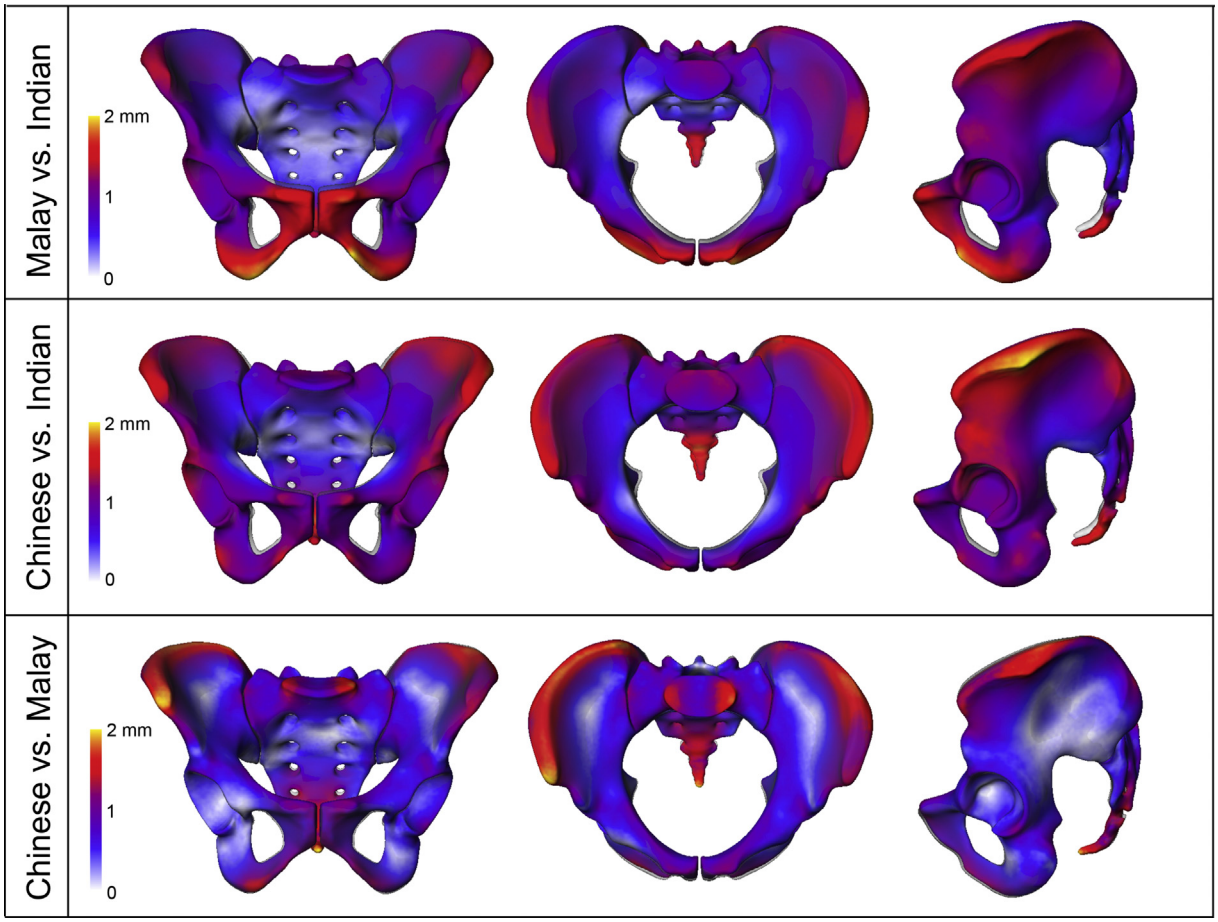

Figure 4. Qualitative and quantitative comparison of the distances between homologous points of the ethnicity-specific models: Malay (coloured) vs. Indian (transparent), Chinese (coloured) vs. Indian (transparent), Chinese (coloured) vs. Malay (transparent). The colour map illustrates the differences of the distances in mm. Overall, the differences are very small with maximum distances around 2 mm (yellow) at the iliac crest.

mean is replaced by the reference mesh. We calculated an overall Asian mean model; specific models for gender (female and male) and ethnicity (Chinese, Malay, Indian) were computed via data grouping.

Analysis

Shape and size variation of the unisex 3D statistical form model of the pelvis were evaluated via PCA using MATLAB software (R2017a, 64-bit, The MathWorks, Bern, Switzerland) [20]. The size variability in the first principal component (PC 1), the second principal component (PC 2) and third principal component (PC 3) was analysed by extracting PC 1, PC 2 and PC 3 form coordinates and correlating them to Frobenius norm, a computational size measure described by Kamer et al. [20].

Using Amira's standard 3D distance measurement and colour mapping tool, shape differences between the gender-specific Asian submodels, as well as between the overall Asian mean model and the preexisting artificial bone model, were analysed. The data of the preexisting ABM is based on a reproduction of a human Caucasian male skeletal (body height approximately 170–175 cm) from an anatomic exhibition (Synbone®, pelvic bone model no. 4060).

We measured the distance between the anterior superior iliac spines (ASIS), between the anterior inferior iliac spines (AIIS), between the promontory and symphysis (conjugate vera, CV) and between the ischial spines (diameter transversa, DT) to quantify length variations of the preexisting ABM, the mean models and for each individual pelvic bone (see Figure A1). Normal distribution was tested using the Shapiro–Wilk Test. Differences in distances (ASIS, AIIS, CV, DT) between the genders of Asians were statistically tested using the Mann–Whitney U test for non-normally distributed data or the unpaired t-test in normally distributed data. Differences between the included three ethnicities were assessed using one-way analysis of variance. Post hoc comparisons were made using the Tukey–Kramer test. Differences between the overall Asian model and the former ABM were analysed using the one sample t-test or one sample Wilcoxon signed rank test depending on data distribution. $P < 0.05$ was considered as significant.

Sample size estimation (leave-one-out test)

To estimate the number of CT scans to be acquired, we performed a sample size estimation using leave-one-out tests according to a method as described by Lamecker et al. [21]. Leave-one-out testing involved computing a series of statistical pelvic form models with an increasing size of training set. Each of the left-out surfaces was reconstructed as accurately as possible by a statistical form model created without this left-out surface. As fitness measure of the reconstruction process, we computed the maximal distance, the mean distance, the median distance and the corresponding standard deviation of all vertices of the left-out surface and the reconstructed surface. Mean distance calculations were characterised by the following CT numbers: for n = 10 CTs, 5.24 ± 2.62 mm; for n = 30 CTs, 3.78 ± 1.7 mm; for n = 50 CTs, 3.17 ± 1.62 mm; for n = 70, CTs: 2.79 ± 1.43 mm; and for n = 100 CTs, 2.38 ± 1.22 mm. Finally, these averaged statistics of all left-out surfaces of the given training set were plotted against the size of the training sets. An increasing number of CT samples included in the 3D statistical form modelling process resulted in a slowly converging line curve with decreasing averaged distances (see Figure A2).

Table 2
Anatomical measurements of the different Asian mean models, the individual bone measurements and lengths differences to the pre-existing bone model ([#]Unpaired t-test, [§]Mann–Whitney U test, °ANOVA with Tukey–Kramer post hoc test).

Mean models	ASIS	AIIS	Conjugate vera	Ischial spine distance
Female pelvic mean model	22.5 ± 2.0 cm range: 17.8–26.5	18.5 ± 1.1 cm range: 16.1–20.6	11.6 ± 1.0 cm range: 9.0–14.0	10.5 ± 0.7 cm range: 8.8–11.9
Male pelvic mean model	22.7 ± 1.3 cm range: 19.2–26.0	18.7 ± 1.0 cm range: 16.2–20.8	10.5 ± 1.0 cm range: 8.4–14.2	8.8 ± 0.8 cm range: 7.0–10.7
	P = 0.4153[#]	*P = 0.3982*[#]	*P < 0.0001*	*P < 0.0001*
Chinese	23.1 ± 1.6 cm range: 19.5–26.3	18.8 ± 1.2 cm range: 16.1–20.8	11.1 ± 1.4 cm range: 8.4–14.3	9.9 ± 1.0 cm range: 8.2–11.9
Indian	22.0 ± 1.4 cm range: 19.2–24.4	18.3 ± 1.0 cm range: 16.2–20.6	10.8 ± 1.1 cm range: 8.8–14.0	9.3 ± 1.2 cm range: 7.0–11.9
Malay	22.7 ± 1.9 cm range: 17.8–26.5	18.6 ± 1.0 cm range: 16.6–20.6	11.4 ± 1.0 cm range: 9.6–13.9	9.7 ± 1.1 cm range: 9.8–11.5
	P = 0.0332° *Chinese/Indian:* *P = 0.0277* *Chinese/Malay:* *P = 0.6555* *Indian/Malay:* *P = 0.2015*	*P = 0.2284*° *Chinese/Indian:* *P = 0.2035* *Chinese/Malay:* *P = 0.7875* *Indian/Malay:* *P = 0.5466*	*P = 0.1801*° *Chinese/Indian:* *P = 0.6039* *Chinese/Malay:* *P = 0.6277* *Indian/Malay:* *P = 0.1535*	*P = 0.0413*° *Chinese/Indian:* *P = 0.0408* *Chinese/Malay:* *P = 0.8277* *Indian/Malay:* *P = 0.1551*
Overall Asian pelvic mean model	22.6 ± 1.7 cm range: 17.8–26.5	18.6 ± 1.1 cm range: 16.1–20.8	11.1 ± 1.2 cm range: 8.4–14.2	9.7 ± 1.1 cm range: 7.0–11.9
Pre-existing artificial bone model	27.5 cm *P < 0.0001*[#]	20.9 cm *P < 0.0001*[#]	10.5 cm *P < 0.0001*[§]	9.5 cm *P = 0.6927*[#]

ASIS, anterior superior iliac spines; AIIS, anterior inferior iliac spines; ANOVA, analysis of variance.

Results

Variation of all 100 pelvic surfaces

PCA demonstrated a high variation of pelvic surfaces (Figure 2). PC 1 comprised 24% of the total anatomical variation and predominantly displayed size variation, especially of the innominate bones. PC 2 mainly exhibited anatomical variations of the relation between the sacral bone and the innominate bones as well as shape variations of the pelvic inlet (+3SD round pelvic inlet and wide distance between sacrum and acetabulum in the lateral view, -3SD oval pelvic inlet and close distance between sacrum and acetabulum in the lateral view). PC 2 and PC 3 contributed less to the total anatomical variation (PC 2: 17.7%, PC 3: 9.7%) and predominantly displayed shape variation. We also observed a notable change specifically in PC 3 of the anteroposterior position of the sacrum with regard to the innominate bones as well as shape variations of the iliac wings (+3SD steep iliac wings, -3SD wide, overhanging iliac wings). PC 1 to PC 3 contained 51.4% of the anatomical variation. PC 1 form coordinates highly correlated with Frobenius norm ($r^2 = 0.95$, $p < 0.0001$). Gender correlated with the form coordinates in PC 2 ($r^2 = 0.81$, $p < 0.0001$).

3D distance mapping of gender- and ethnicity-specific mean models

3D distance mapping demonstrated different distances between both genders, especially in the iliac wing, the pubic bone, the arcuate line, the acetabulum, and the ischial spines (Figure 3a). Differences between the ethnicities are shown in Figure 4; only small differences were found with maximal distances of 2 mm, for example, at the iliac crest (coloured yellow).

Distance measurements

ASIS and AIIS (external linear measurements) were measured in the female and male pelvic mean model as well as in the pre-existing bone model. These measurements remained nearly identical for both genders, whereas conjugate vera and ischial spine distance (internal linear measurements) were notably different (Table 2). Significant, but small, differences were found between the ethnicities regarding ASIS and ischial spine distance as smaller distances were found between Chinese and Indian.

Comparison of the overall mean model with pre-existing pelvic bone model (Synbone pelvic model no. 4060)

The two internal pelvic measurements of conjugate vera and ischial spine distance varied with 0.6 cm and 0.5 cm, respectively. Differences between the overall Asian mean model and the pre-existing bone model are displayed in Figure 3b and linear measurements were summarised in Table 2. The external pelvic linear measurements ASIS and AIIS were markedly different. All one-hundred individual Asian bone models demonstrated smaller ASIS and AIIS measurements than the pre-existing pelvic bone model.

Model manufacturing

An ABM was manufactured of the mean model of the 50 male pelvic surfaces and an anatomical variation of the female mean pelvic surface, the latter missing a trans-sacral corridor S1, thus preventing the placement of trans-sacral implants. This female pelvis was sampled from the 3D statistical form model created with 50 female pelvis surfaces as a training set. ABMs were refined to create surface roughness analogous to that of the natural pelvis. ABMs were manufactured (Synbone AG, Malans, Switzerland) from specially formulated polyurethane foam comprising a cancellous inner core and a harder outer shell simulating cortical bone (see Figure 5).

Discussion

The analyses demonstrated notable interindividual anatomical variations regarding the pelvic shape and size. PCA assessed the complex anatomy of the three ring-building bones of the pelvis. As expected, PC 1 contained most of the anatomical variation and predominantly demonstrated a size variation. However, PC 1 explained only 24% of the anatomical variation and was highly correlated with the pelvic size as analysed by the Frobenius norm. The high correlation of size with PC 1 was also observed in other statistical models of human bones, demonstrating size to be the most important variation [22,23]. PC 2 consisted of variations in the distance between sacrum and acetabulum as well as the

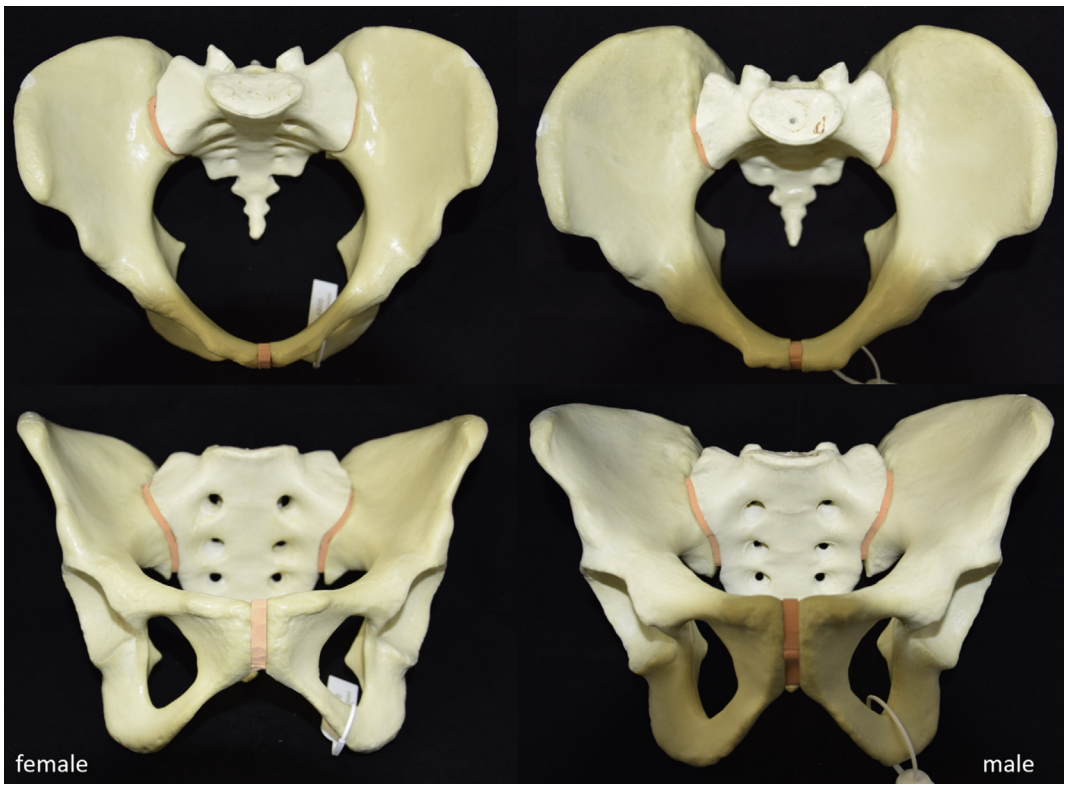

Figure 5. Gender-specific Asian mean models manufactured by Synbone AG, Malans, Switzerland using specially formulated polyurethane foam (left: female model with missing bony S1 corridor; right: male mean model).

shape of the pelvic inlet. The variation in PC 2 was mostly explained by gender differences. The explained variation using the PC 1 and PC 2 was smaller compared with long bones (e.g., Caucasian humerus: 65% [22]). This emphasises the difficulties in depicting the individual anatomy of the pelvic ring compared with other bones.

Recently, a 3D statistical mean model of the pelvic bone consisting of 50 Japanese was published [18]. PCA of the Japanese statistical pelvic bone model predominantly showed size variation (PC 1: 20.4%) followed by shape variation (PC 2: 14.1%) similar to the PCA of the present study. In addition, the linear measurements of the internal pelvic parameter of the Japanese model were very similar to the models (Chinese, Malay, Indian) presented in our study. The distance between promontory and symphysis was 11.1 cm, the ischial spine distance was 9.8 cm. Differences compared with our models were found for the ASIS (23.8 cm), whereas the AIIS was similar (19.0 cm).

We observed major differences in linear measurements between the Asian pelvic mean model and the pre-existing artificial bone model. The external pelvic linear measurements ASIS and AIIS (ASIS difference = 4.9 cm; AIIS difference = 2.3 cm) differed especially largely. All of the one-hundred individual Asian bone models demonstrated smaller ASIS and AIIS measurements than the pre-existing pelvic bone model. Previously, other authors have attributed bone shape differences in the spine and the pelvic region to ethnic origin [9,10,12].

These anatomical differences can have important implications for trauma surgery and osteosynthesis of fractures. Studies by Ji et al. [24] and Bi et al. [25] on Chinese pelvises found gender-specific differences in the safe angles of screw placement at the superior and inferior border of the arcuate line for the treatment of the acetabular fractures. As demonstrated by Wagner at al. [26], the human sacrum size and shape is highly variable, affecting the size and availability of the trans-sacral corridor S1. Therefore, safe trans-sacral implant positioning on the level of S1 is often but not always possible because of interindividual anatomical differences [16]. The prevalence of dysmorphic sacra limiting S1 trans-sacral screw implantation was reported to be approximately 35% [27], with higher prevalence in females [12,28] and Asian ethnicities [12,29].

To the best of our knowledge, this is the first investigation reporting on generic Asian pelvic bone model fabrication. To manufacture ethnicity-specific ABMs, several criteria were required to be considered for integration into the modelling, analysis, and fabrication process. These included the selection of appropriate type and quantity of image data and demographic information, and the usage of suitable data processing techniques, model material and model manufacturing techniques.

CT-based 3D statistical bone modelling is a method that has been derived from geometric morphometrics [19]. Typically, PCA is used to visualise and assess anatomical variation such as 3D size and shape variations, and also to generate a mean model. However, other image data, methodologies, or terms may be applied [30,31]. A total number of one hundred clinical pelvic CT scans were used; these were representative for the Asian population because all pelvic CT data were acquired from Malaysian adults and sampled in equal parts from three major ethnic groups of this area, namely from Chinese, Indian and Malay descent. Significant but small differences were only found between Chinese and Indian regarding the ASIS and the ischial spine distance.

Additional demographic information comprises records about age, gender, body height and weight, which were all comparable with epidemiological studies [32]. Sample size estimation was made using leave-one-out tests according to a method described by Lamecker [21]. They exhibited a slowly converging line curve, with decreasing values for maximum distances, mean distances, standard deviation and median distances between homologous anatomical surface points of the mean models. As shown by the slowly converging curve, relevant improvements of the statistical form model can only be made with much more pelvis sample in the training set. Therefore, we considered a sample of 100 pelvic CT samples to be sufficient for data grouping according to gender, and no more CT samples were required to refine our study results.

ABMs are commonly used for teaching the principles of fracture fixation, fracture reduction and osteosynthesis techniques [33] and are based on image data of one individual. An important difference is that our ABM was the result of a mean model, representing the anatomy of the Asian population better. By showing large anatomic variation between the former and the new bone models, we cannot conclude that the education and the knowledge improves by using the Asian model in the future, nor that it has implications for the patient treatment and surgical outcomes. Hands-on experience, familiarity with orthopaedic instruments and proficiency in the different steps of the surgery can be gained with both bone models. However, the manufactured novel ABMs depict the neuroforamina with the sacral canal which has not been manufactured for educational purposes before. Moreover, a female Asian pelvic bone model with a missing trans-sacral corridor S1 was manufactured, and such a model reflects the overproportional prevalence of this anatomical variation from the common pelvic shape seen in the Asian population and in female gender [12,26,28,29]. This is very useful for training and education as no direct trans-sacral fixation is possible in this model. Therefore, the trainees can learn better how to deal with such a problem, such as by placement of a trans-sacral implant at S2 level.

In conclusion, we used a robust number of pelvic CTs of adult Asian patients and CT-based 3D statistical modelling to reveal notable anatomical variations, with size variation dominating over shape and gender-specific variability. Dimensions of the generated mean models were comparatively smaller than the pre-existing ABM. This highlights the necessity to generate Asian ABMs by evidence-based modeling techniques to match the anatomical characteristics of the growing Asian population.

Conflicts of interest

The authors declare that they have no conflict of interest.

Acknowledgements

The authors are not compensated and there are no other institutional subsidies, corporate affiliations, or funding sources supporting this work unless clearly documented and disclosed. This investigation was performed with the assistance of the AO Foundation and funded via the AO Strategy Fund (Project No. 58: Generic Asian Pelvic Bone Model).

Authors' contributions: MA, HN, and LK contributed to data processing, data analysis and calculations of the three-dimensional models. KS and TKZ performed the data acquisition and preparation of the CT scans for further usage. FB and AN manufactured the artificial bone models and developed a concept to do so. GR, BG, AN and TKZ contributed substantially to the research design, and the data analysis and presentation. MA drafted the manuscript with the help of LK and HN. BG and GR revised it critically. All listed authors approved the submission of the final version of the manuscript.

Appendix A. Supplementary data

Supplementary data to this article can be found online at https://doi.org/10.1016/j.jot.2019.10.004.

References

[1] Spiegel DA, Gosselin RA, Coughlin RR, Joshipura M, Browner BD, Dormans JP. The burden of musculoskeletal injury in low and middle-income countries: challenges and opportunities. JBJS 2008;90(4):915–23.
[2] Injuries WHO, Department VP. The injury chart book: a graphical overview of the global burden of injuries. World Health Organization; 2002.
[3] Shim V, Boheme J, Josten C, Anderson I. Use of polyurethane foam in orthopaedic biomechanical experimentation and simulation. In: Polyurethane. InTech; 2012. p. 171–200.
[4] Elfar J, Stanbury S, Menorca RMG, Reed JD. Composite bone models in orthopaedic surgery research and education. J Am Acad Orthop Surg 2014;22(2):111.
[5] Atesok K, Mabrey JD, Jazrawi LM, Egol KA. Surgical simulation in orthopaedic skills training. JAAOS-J Am Acad Orthop Surg 2012;20(7):410–22.
[6] Anastakis DJ, Regehr G, Reznick RK, Cusimano M, Murnaghan J, Brown M, et al. Assessment of technical skills transfer from the bench training model to the human model. Am J Surg 1999;177(2):167–70.
[7] Singh A, Sharma R, Sharma R, Musmade D. Challenges in cadaver availability for learning and research in medical sciences. Int J Med Clin Res 2011;2(2):67–71.
[8] Peng S, Linan Z, Zengtao H, Xueling B, Xin Y, Zhaobin X, et al. Morphometric measurement of the patella on 3D model reconstructed from CT scan images for the southern Chinese population. Chin Med J 2014;127(1):96–101.
[9] Hoaglund F, Low WD. Anatomy of the femoral neck and head, with comparative data from Caucasians and Hong Kong Chinese. Clin Orthop Relat Res 1980;(152):10–6.
[10] Zárate-Kalfópulos B, Romero-Vargas S, Otero-CáMara E, Correa VC, Reyes-Sánchez A. Differences in pelvic parameters among Mexican, Caucasian, and Asian populations. J Neurosurg Spine 2012;16(5):516–9.
[11] Arima H, Dimar JR, Glassman SD, Yamato Y, Matsuyama Y, Mac-Thiong J-M, et al. Differences in lumbar and pelvic parameters among African American, Caucasian and Asian populations. Eur Spine J 2018;27(12):2990–8.
[12] Wagner D, Kamer L, Sawaguchi T, Geoff Richards R, Noser H, Uesugi M, et al. Critical dimensions of trans-sacral corridors assessed by 3D CT models: relevance for implant positioning in fractures of the sacrum. J Orthop Res 2017;35(11):2577–84.
[13] Noser H, Hammer B, Kamer L. A method for assessing 3D shape variations of fuzzy regions and its application on human bony orbits. J Digit Imaging 2010;23(4):422–9.
[14] Kamer L, Noser H, Schramm A, Hammer B. Orbital form analysis: problems with design and positioning of precontoured orbital implants: a serial study using post-processed clinical CT data in unaffected orbits. Int J Oral Maxillofac Surg 2010;39(7):666–72.
[15] Noser H, Heldstab T, Schmutz B, Kamer L. Typical accuracy and quality control of a process for creating CT-based virtual bone models. J Digit Imaging 2011;24(3):437–45.
[16] Wagner D, Kamer L, Rommens PM, Sawaguchi T, Richards RG, Noser H. 3D statistical modeling techniques to investigate the anatomy of the sacrum, its bone mass distribution, and the trans-sacral corridors. J Orthop Res 2014;32(11):1543–8.
[17] Wagner D, Kamer L, Sawaguchi T, Richards RG, Noser H, Rommens PM. Sacral bone mass distribution assessed by averaged three-dimensional CT models: implications for pathogenesis and treatment of fragility fractures of the sacrum. JBJS 2016;98(7):584–90.
[18] Arand C, Wagner D, Richards RG, Noser H, Kamer L, Sawaguchi T, et al. 3D statistical model of the pelvic ring–a CT-based statistical evaluation of anatomical variation. J Anat 2019;234(3):376–83.
[19] Bookstein FL. Morphometric tools for landmark data: geometry and biology. Cambridge University Press; 1997.
[20] Kamer L, Noser H, Hammer B. Anatomical background for the development of preformed cranioplasty implants. J Craniofac Surg 2013;24(1):264–8.
[21] Lamecker H, Kamer L, Wittmers A, Zachow S, Kaup T, Schramm A, et al. A method for the three-dimensional statistical shape analysis of the bony orbit. Proc Computer Aided Surgery Around the Head 2007:94–7.
[22] Kamer L, Noser H, Popp AW, Lenz M, Blauth M. Computational anatomy of the proximal humerus: an ex vivo high-resolution peripheral quantitative computed tomography study. J Orthop Transl 2016;4:46–56.
[23] Kamer L, Noser H, Blauth M, Lenz M, Windolf M, Popp AW. Bone mass distribution of the distal tibia in normal, osteopenic, and osteoporotic conditions: an ex vivo assessment using HR-pQCT, DXA, and computational modelling. Calcif Tissue Int 2016;99(6):588–97.
[24] Ji X, Bi C, Wang F, Jiang Y, Wang D, Wang Q. Digital anatomical measurements of safe screw placement at superior border of the arcuate line for acetabular fractures. BMC Muscoskelet Disord 2015;16(1):55.
[25] Bi C, Wang J, Ji X, Ma Z, Wang F, Zeng X, et al. The safe screw path along inferior border of the arcuate line at acetabular area: an anatomical study based on CT scans. BMC Muscoskelet Disord 2017;18(1):88.
[26] Wagner D, Kamer L, Sawaguchi T, Richards RG, Noser H, Hofmann A, et al. Morphometry of the sacrum and its implication on trans-sacral corridors using a computed tomography data-based three-dimensional statistical model. Spine J 2017;17(8):1141–7. https://doi.org/10.1016/j.spinee.2017.03.023.
[27] Chip Jr MC, Simonian PT, Agnew SG, Mann FA. Radiographic recognition of the sacral alar slope for optimal placement of iliosacral screws: a cadaveric and clinical study. J Orthop Trauma 1996;10(3):171–7.
[28] Lee JJ, Rosenbaum SL, Martusiewicz A, Holcombe SA, Wang SC, Goulet JA. Transsacral screw safe zone size by sacral segmentation variations. J Orthop Res 2015;33(2):277–82.
[29] Kaiser SP, Gardner MJ, Liu J, Routt Jr MC, Morshed S. Anatomic determinants of sacral dysmorphism and implications for safe iliosacral screw placement. JBJS 2014;96(14):e120.
[30] Mitteroecker P, Gunz P, Windhager S, Schaefer K. A brief review of shape, form, and allometry in geometric morphometrics, with applications to human facial morphology. Hystrix Ital J Mammal 2013;24(1):59–66.
[31] Klingenberg CP. Size, shape, and form: concepts of allometry in geometric morphometrics. Dev Gene Evol 2016;226(3):113–37.
[32] Lim T, Ding L, Zaki M, Suleiman A, Fatimah S, Siti S, et al. Distribution of body weight, height and body mass index in a national sample of Malaysian adults. Med J Malays 2000;55(1):108–28.
[33] Buckley Richard E, Moran Christopher G, Apivatthakakul T. AO principles of fracture management. 3rd ed. ed 2018.